

Ba termination of Ge(001) studied with STM

This content has been downloaded from IOPscience. Please scroll down to see the full text.

2015 Nanotechnology 26 155701

(<http://iopscience.iop.org/0957-4484/26/15/155701>)

View [the table of contents for this issue](#), or go to the [journal homepage](#) for more

Download details:

IP Address: 144.82.107.165

This content was downloaded on 03/11/2015 at 13:53

Please note that [terms and conditions apply](#).

Ba termination of Ge(001) studied with STM

W Koczorowski^{1,2}, T Grzela³, M W Radny^{2,4}, S R Schofield^{1,5}, G Capellini^{3,6},
R Czajka², T Schroeder^{3,7} and N J Curson⁸

¹ London Centre for Nanotechnology, University College London, 17-19 Gordon Street, London, UK

² Institute of Physics, Poznan University of Technology, ul. Piotrowo 3, 60-965 Poznan, Poland

³ IHP, Im Technologiepark 25, D-15236 Frankfurt (Oder), Germany

⁴ School of Mathematical and Physical Sciences, The University of Newcastle, Callaghan 2308, Australia

⁵ Department of Physics and Astronomy, UCL, London, WC1E 6BT, UK

⁶ Dipartimento di Scienze, Università degli Studi Roma Tre, I-00146 Roma, Italy

⁷ BTU Cottbus, Konrad-Zuse Str. 1, D-03046 Cottbus, Germany

⁸ Department of Electronic and Electrical Engineering, UCL, London, WC1E 7JE, UK

E-mail: wojciech.koczorowski@put.poznan.pl and n.curson@ucl.ac.uk

Received 2 November 2014, revised 6 February 2015

Accepted for publication 14 February 2015

Published 23 March 2015



CrossMark

Abstract

We use controlled annealing to tune the interfacial properties of a sub-monolayer and monolayer coverages of Ba atoms deposited on Ge(001), enabling the generation of either of two fundamentally distinct interfacial phases, as revealed by scanning tunneling microscopy. Firstly we identify the two key structural phases associated with this adsorption system, namely on-top adsorption and surface alloy formation, by performing a deposition and annealing experiment at a coverage low enough (~ 0.15 ML) that isolated Ba-related features can be individually resolved. Subsequently we investigate the monolayer coverage case, of interest for passivation schemes of future Ge based devices, for which we find that the thermal evaporation of Ba onto a Ge(001) surface at room temperature results in on-top adsorption. This separation (lack of intermixing) between Ba and Ge layers is retained through successive annealing steps to temperatures of 470, 570, 670 and 770 K although a gradual ordering of the Ba layer is observed at 570 K and above, accompanied by a decrease in Ba layer density. Annealing above 770 K produces the 2D surface alloy phase accompanied by strain relief through monolayer height trench formation. An annealing temperature of 1070 K sees a further change in surface morphology but retention of the 2D surface alloy characteristic. These results are discussed in view of their possible implications for future semiconductor integrated circuit technology.

Keywords: STM, barium, Ge(001)


(Some figures may appear in colour only in the online journal)

1. Introduction

The integration of germanium (Ge) into silicon (Si) micro- and nano-electronics is an important materials science approach to further extend the performance and functionality of group IV semiconductor integrated circuit technology [1]. In the field of ‘More Moore’ research and development, further scaling of metal–oxide semiconductor field effect

transistors (MOSFETs) calls for alternative high mobility channel materials. Ge is considered to be a ‘hot candidate’ material for setting up p-channel transistors due to its higher hole mobility and hole concentration than in Si or the III–V semiconductors [2]. In the area of ‘More than Moore’ research, active Ge photonic devices like photodetectors [3, 4], modulators [5] and even lasers [6] are intensively investigated to set up electronic–photonic integrated circuits mainly because the Ge band gap value perfectly matches standard telecommunication wavelengths [7].

A key element in both ‘More Moore’ and ‘More than Moore’ approaches is the control over Ge surface chemistry and physics. Indeed surface chemical and electronic

 Content from this work may be used under the terms of the Creative Commons Attribution 3.0 licence. Any further distribution of this work must maintain attribution to the author(s) and the title of the work, journal citation and DOI.

passivation by gate dielectrics on Ge FETs must be controlled at the atomic scale in order to provide an effective oxidation barrier to prevent GeO_x formation and to guarantee low current leakage and low interface trap densities [8, 9]. Surface passivation is also of central importance for the control of surface recombination effects in Ge photonic devices [10, 11]. Of equal importance is the ability to achieve low resistance metal contacts to Ge, especially when high current densities need to be applied, e.g., in Ge MOSFETs and Ge laser diodes [12–14]. In particular, it is known that Fermi level pinning of Ge(001) surfaces leads to a requirement for special surface passivation schemes for the formation of low resistance ohmic contacts to *n*-type Ge(001) [15].

Alkaline earth metal adlayers were reported to exhibit interesting passivation properties on Si(001) but to date there has been relatively little work devoted to the increasingly important Ge(001) surface. For example, Sr and Ba adlayers on Si(001) achieved a strong suppression of parasitic Si oxidation and enabled the growth of functional hetero-epitaxial SrTiO_3 or BaTiO_3 perovskite thin films [16–19]. Thus, based on the ratio of atomic radii of Sr/Si(001), the Ba/Ge(001) system was suggested as an alkaline earth template for subsequent BaTiO_3 growth on Ge [18–20]. The BaTiO_3 /Ge system is expected to be less critical than the SrTiO_3 /Si system in terms of interface reactivity at the early stages of the growth [21]. However, it is well known that subtle energy and band structure differences between Si(001) and Ge(001) [22] result in a rather complex interface between alkaline earth metal adlayers, necessitating more detailed studies exploring the potential of Ba on Ge(001) for passivation applications. One study of the Ba/Ge(001) system was performed by Cattoni *et al* [23] who investigated the growth of Ba overlayers using LEED, UPS, and XPS. They concluded that at coverage of 1.2 and 1.5 ML the order of Ba on Ge(001) is different to that observed for Sr on Si(001), and that the presence of Ba on the Ge(001) surface at the reported experimental conditions increases its oxidation tendency. Up until now, systematic scanning tunneling microscopy (STM) studies on alkaline earth metals on Ge(001) focused mostly on Sr [20, 24, 25] and very little effort has been devoted to Ba [20]. Important experiments which guided the initial direction of the research presented here come from an STM study of the similar Ba/Si(001) system [26]. Here the adsorption of <1/6 ML of Ba on Si(001) at 900 °C showed the formation of co-existing features with the appearance of nanolines and of protrusions-in-troughs which were interpreted as originating from Ba adsorbed on top of the Si(001) surface and of Ba incorporation into the Si(001) surface layer, respectively.

In this paper, we use STM to study the Ba/Ge(001) interface in detail. We first characterize the Ge(001) surface after the deposition of ~0.15 ML of Ba at room temperature (RT) and then after the sample was annealed to 770 K for 30 min, allowing us to identify the two key structural phases associated with this adsorption system, namely on-top adsorption and surface alloy formation, as we expected from comparison with the Ba/Si(001) adsorption system [26]. Then, in order to mimic a typical processing step in micro- and nanoelectronics, we studied one monolayer of Ba on Ge

(001) deposited at RT and explored its structural changes over the range of temperature (RT to 1070 K) which can in principle be applied for Ge device processing.

2. Experiment

Experiments were performed in a commercial Omicron Nanotechnology ultra-high vacuum (UHV) STM system (XA variable temperature head) with a base pressure $<5 \times 10^{-11}$ mbar. Ge(001) samples (3×8 mm) were cleaved from an Sb-doped wafer ($1 \sim 10 \Omega\text{cm}$) and mounted on a direct current heating sample holder. Clean, reconstructed Ge(001) surfaces were obtained by several cycles of Ar^+ ion sputtering for 30 min (energy 0.75 keV, emission current 10 mA, Ar pressure 10^{-5} mbar), followed by annealing steps at 1070 K for 5 min and 970 K for 15 min, within the UHV preparation chamber [27]. By this procedure, $p(2 \times 1)$ and $c(4 \times 2)$ reconstructions of the Ge(001) surface were the dominating surface phases at RT, with dimer vacancy concentration estimated to be ~3%. The Ba layer was deposited at RT, followed by various subsequent annealing steps in the temperature range from 470 up to 770 K for 30 min using radiative heating and from 870 to 1070 K for 10 min, by means of direct heating. The substrate temperature was measured using a thermocouple mounted on the preparation stage, which was in direct contact with the sample holder, and assisted by the use of an infrared pyrometer. Ba was evaporated onto the surface by means of an Omicron Nanotechnology EFM-3 e-beam evaporator with a Mo crucible, using an ion current flux of ~10 nA and an electron energy 500 V. STM images were taken at 100 K, using electrochemically etched tungsten tips and data processing was carried out using the WSxM software [28]. Coverage calibration was achieved by using STM to count the number of surface features as a function of deposition time for sub monolayer coverage deposition times, and then extrapolating for higher coverages.

3. Results and discussion

A key finding of this paper is the determination of two important phases of the Ba/Ge(001) interface, which we have achieved by imaging sub-monolayer Ba coverages. Figures 1(a)–(c) show a Ge(001) surface where we have deposited ~0.15 ML Ba at RT. Figure 1(a) shows a $75 \times 75 \text{ nm}^2$ STM image of two terraces, and just a small part of a third one (at the bottom right of the image), separated by atomic steps that run from bottom-left to top-right in the image. Rows of Ge surface dimer atoms run in the [1–10] direction on the top terrace and in the [110] direction on the terrace below. The Ba-induced features appear as brighter meandering lines on top of the terraces that we refer to henceforth as nanolines. On the upper terrace these nanolines are observed to be oriented along the [310] and/or [130] surface directions and rarely along [-110]. On the lower terrace nanolines are formed along [-310] and/or [-130], and less

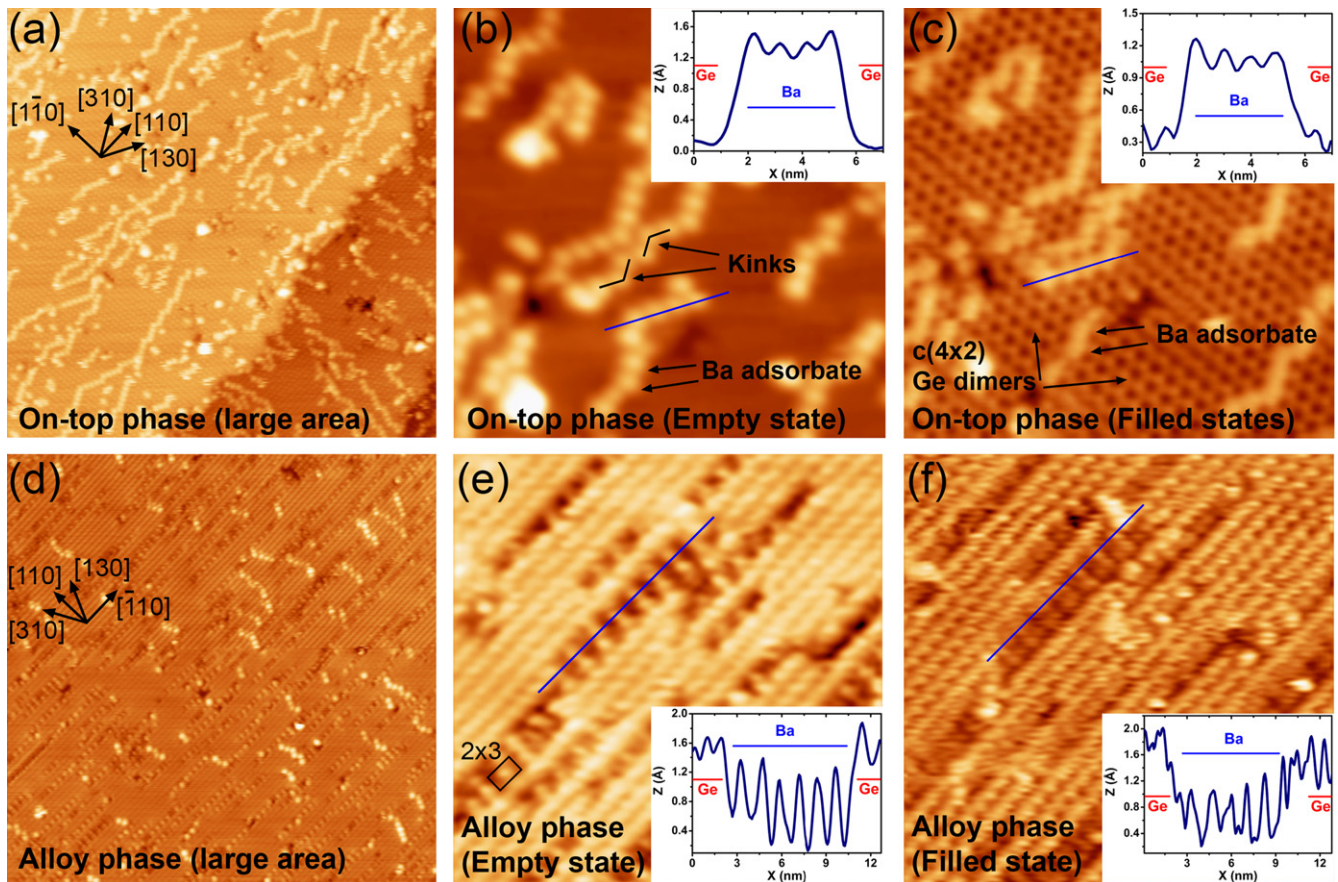


Figure 1. (a)–(c) show STM images of the Ge(001) surface after the deposition of ~ 0.15 ML of Ba at room temperature taken at a tunneling current of $I = 20$ pA and sample biases of $V_s = 2, 2$ and -2 V respectively. (a) is 75×75 nm², (b) and (c) are 20×20 nm². Images reveal the on-top adsorption phase. (d)–(f) Show STM images of the surface after annealing to 770 K for 30 min, taken at $I = 1$ nA and $V_s = 1.5, 1$ and -1 V respectively, revealing the 2D surface alloy phase. (d) is 75×75 nm², (e) and (f) are 20×20 nm². The insets in (b), (c), (e) and (f) show height profiles obtained along the segments of the images highlighted by the blue lines. The rectangular box in (e) shows the 2×3 surface unit cell of the incorporated Ba.

frequently in the $[110]$ surface directions. Moreover most of the formed nanolines contain many kinks giving them a zigzag appearance. Figures 1(b) and (c) show empty state and filled state (respectively) higher resolution images (20×20 nm²) of the same area of another part of the surface, where individual features can be clearly resolved and the kinks are highlighted. Cross-sections taken from the images (see insets) reveal the nanolines have an apparent height of 0.12 ± 0.02 nm which compares with the measured apparent height of a Ge atomic step of 0.14 ± 0.02 nm, indicating that the nanolines are approximately 1 atom high. However, the structures of the nanolines themselves bare no resemblance to epitaxial Ge rows. In figure 1(c) the $c(4 \times 2)$ structure of the underlying Ge(001) surface is clearly resolved and there is no evidence of the nanolines altering the surface reconstruction, as highlighted by the two areas of $c(4 \times 2)$ reconstruction labelled in the figure. The observed nanolines are similar to those formed after the adsorption of Ba on the Si(001) surface at 900°C [26]. A reasonable conclusion to draw from these observations, and the fact that the Ba deposition was performed at RT where the Ge(001) surface is known to be stable, is that the nanolines are formed from Ba adsorbates adsorbed on top of the Ge(001) surface with no atomic

intermixing between the Ba and Ge. Other similar systems where ‘on-top’ adsorption does not lead to significant substrate modification are Ba/Si(001) [29] and Li/K/Si(001) [30].

Figures 1(d)–(f) show a different area of the same surface that is shown in figures 1(a)–(c), after the sample has been annealed for 30 min at 770 K. It can be readily observed that the appearance of the surface has been radically altered by the annealing process. All figures 1(d)–(f) show a single terrace with the Ge dimers running in the $[-110]$ direction of the surface. The nanolines have almost completely disappeared, and they have been replaced with circular features that reside inside long rectangular depressions running along the Ge dimer row direction. We refer to these features henceforth as ‘protrusions-in-troughs’. The insets in figures 1(e) and (f) shows a cross-section obtained along a Ge dimer row containing protrusions-in-troughs. The separation between the bright protrusions is 1.22 ± 0.08 nm in the dimer row direction. The apparent height difference clearly shows that the protrusions-in-troughs cannot originate from the ‘on-top’ adsorption of Ba atoms on the dimerized Ge surface, what is also visible in figure 1(f). The different apparent heights and directions of Ba induced structures confirm the alloy phase formation. We propose therefore that the protrusions are Ba

adatoms that have been thermally incorporated into the surface such that they can be considered adatoms of the second layer Ge atoms. Our assignment is similar to that made in the study of low coverage Ba adsorption on Si(001) at an adsorption temperature of 900 °C [26]. Close inspection of figures 1(e) and (f) also show that in several cases two rows of protrusions-in-troughs run parallel to one another along neighbouring dimer rows with the bright protrusions in phase. As a consequence, structures consisting of pairs of the protrusions are formed, with a 2×3 surface unit cell in the [110] and $[-110]$ surface directions, respectively, highlighted in figure 1(e). The same periodicities of the alkaline earth induced surface structures were observed to be dominant on Si(001) e.g. Sr/Si(001) and Ba/Si(001) [11, 26]. The adatom induced 2×3 periodicity on Ge(001) was also observed after evaporating $\sim 1/6$ ML Sr on the Ge(001) substrate kept at 675 K [20]. We refer to this annealed surface (figures 1(d) and (f)) as the *2D surface alloy phase* which we have identified in distinct contrast to the *on-top adsorption* phase seen in figures 1(a)–(c). So what we have done so far is to study the Ba/Ge(001) interface at low Ba coverage in order to straightforwardly benchmark two critical surface phases at separate temperatures, to which we will refer later in the paper.

We now describe the formation of the Ba adstructures at the coverage of one monolayer of Ba atoms on Ge(001), of interest for passivation schemes of future Ge based devices. We note that the coverage of 1 ML corresponds to a 1:1 ratio between deposited Ba and Ge surface atoms and since the covalent radii of Ba is 198 pm compare to Ge of 121 pm [31] we expect the layer to actually form slightly more than a complete single covering layer of surface atoms. Our starting point is the clean Ge(001) surface shown in the 75×75 nm² filled state STM image of figure 2(a). The image shows two terraces separated by a single monolayer high step running down the centre of the image. The surface is of high quality, largely free of contamination and defects. A coverage of 1 ML of Ba was then deposited onto the sample at RT. An STM image of the surface after deposition is shown in figure 2(b). Here the surface appears to be covered by an inhomogeneous layer of material, which we attribute to randomly distributed Ba clusters whose lateral dimensions are in the range of 1–2 nm, although the underlying Ge terrace structure is still visible in the image. The formation of a second layer of clusters on top of the first layer, is also apparent, resulting from the slight excess of Ba above that required to completely cover the surface, as mentioned above.

We then performed a number of sequential annealing steps at temperatures of 470, 570, 670 and 770 K, each for 30 min. Our STM images revealed no significant change after annealing to 470 K. We show the surface imaged after the 570, 670 and 770 K anneals, in figures 2(c)–(f), respectively, where we see a number of distinct changes to the surface. Firstly we see that as the surface temperature is increased to 570 K there is a decrease in the apparent surface Ba coverage compared to that observed at RT (figure 2(b)), as is evidenced by the fact that the underlying surface can now be seen between many of the surface features in figures 2(c)–(f) i.e.

the adlayer appears to be a more open structure. Furthermore, most of the clusters seen in figure 2(b) have disappeared, to be replaced by individual protrusions of a smaller size, most of which align into nanolines of various lengths, generally consisting of just a few protrusions. It is therefore reasonable to deduce that there is a decrease of the Ba coverage on the surface caused by annealing, most likely associated with the re-evaporation of Ba. We conclude that these nanolines are oriented along the same surface directions shown in the low coverage case of figures 1(a)–(c). The kinks in the nanolines, resulting from changes in directions along which the nanolines run, and which give the nanolines their zigzag appearance, are also highlighted in the inset of figure 2(d) which is a 20×20 nm² image of the 670 K annealed surface. The shortest distance between neighbouring nanolines is 1.6 nm which is equal to $4 \times a$ where a is the surface lattice constant of the ideal Ge(001) surface. These nanolines closely resemble those seen in figures 1(a)–(c).

In the temperature range 570–770 K the apparent surface Ba coverage decreases by approximately 10% for each temperature increase step, as determined by a simple image threshold analysis⁹. Correspondingly a few larger clusters of material form on top of the surface during these annealing steps, reaching 0.1–0.3 nm apparent height, 1–5 nm in diameter and 3% coverage at 770 K. Also associated with the decrease in coverage is an increase in the number of kinks observed in the nanolines, plotted in the inset of figure 2(e) as a ratio of number of kinks/number of Ba adsorbates. An example of a high local kink density is shown in figure 2(f), highlighted by the white rectangle, where a kink exists between every Ba adsorbate producing zigzag chain structure. The correlation between the nanolines seen in figures 2(c)–(f) and those in figures 1(a)–(c) enable us to firmly assign this phase of adsorption to the *on-top adsorption* phase, which enables us to assert that the layer we see after RT adsorption (figure 2(b)) is a Ba overlayer with no significant inter-mixing and subsequent anneal of the sample results in an ordering of the overlayer structure. It is interesting to note that the onset of surface alloy phase formation is observed after annealing at 770 K for lower coverage, as shown in figures 1(d)–(f). This implies that larger Ba coverage stabilizes the Ba overlayer by either suppressing adatom diffusion and/or limiting the reaction sites required for the exchange of Ba and Ge atoms at the interface.

So far we have described the formation of on-top adsorption of a ML of Ba on the Ge(001) surface and the ordering into kinked nanoline structures as a function of increasing temperature to 770 K. When the annealing temperature is increased to 870 K there is a dramatic alteration of the nature of the interface, as is seen in figures 3(a) and (b). On a scale of 400×400 nm² (figure 3(a)) the surface consists of terraces separated by monolayer high steps but with the terraces punctuated with trenches to produce plateaus with

⁹ Threshold analysis was performed on single terraces, with the calculated covered area estimated by defining height interval populations using the flooding function of the WSxM software package. Coverage was calculated for structures higher than 0.7A.

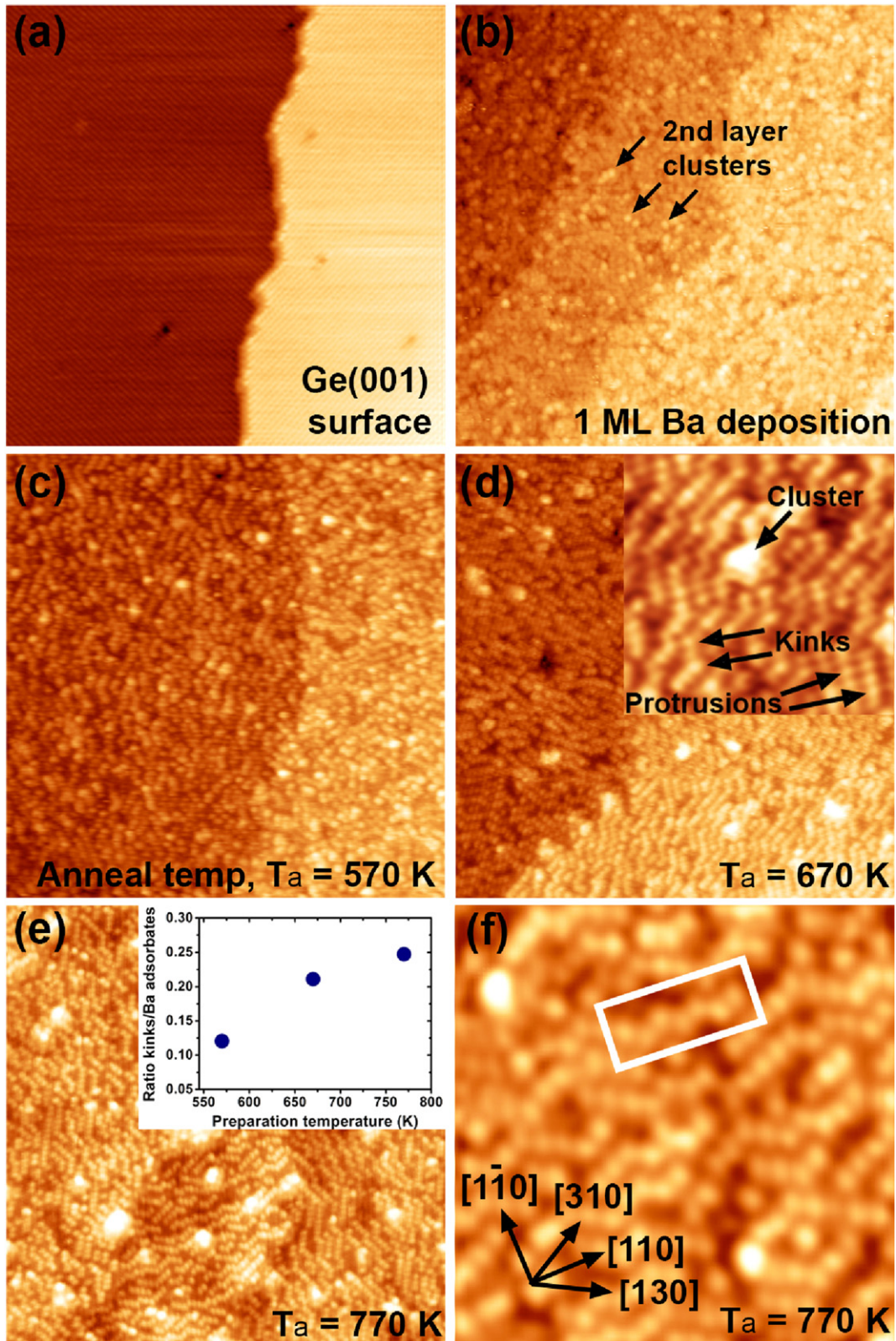


Figure 2. STM images ($75 \times 75 \text{ nm}^2$) showing different areas of a Ge(001) surface (a) before and (b) after the deposition of 1 ML of Ba at room temperature, and the subsequent annealing of the sample to temperatures of (c) 570 K for 30 min, (d) 670 K for 30 min and (e) 770 K for 30 min. The inset in (d) is a magnified area ($20 \times 20 \text{ nm}^2$) of the surface in (d) imaged under the same conditions. (f) is an enlarged area of the surface ($20 \times 20 \text{ nm}^2$) shown in (e). A region of the underlying Ge(001) surface is highlighted by the arrow. Sample biases used were (a) -1.8 V, (b) -2.0 V, (c)–(f) 2.0 V. Imaging currents varied from 80–120 pA. The graph in (e) shows the ratio of the number of kinks to the number of Ba adsorbates for the three sample temperatures shown in (c)–(e). The white rectangle in (f) shows a zigzag chain structure of Ba adsorbates.

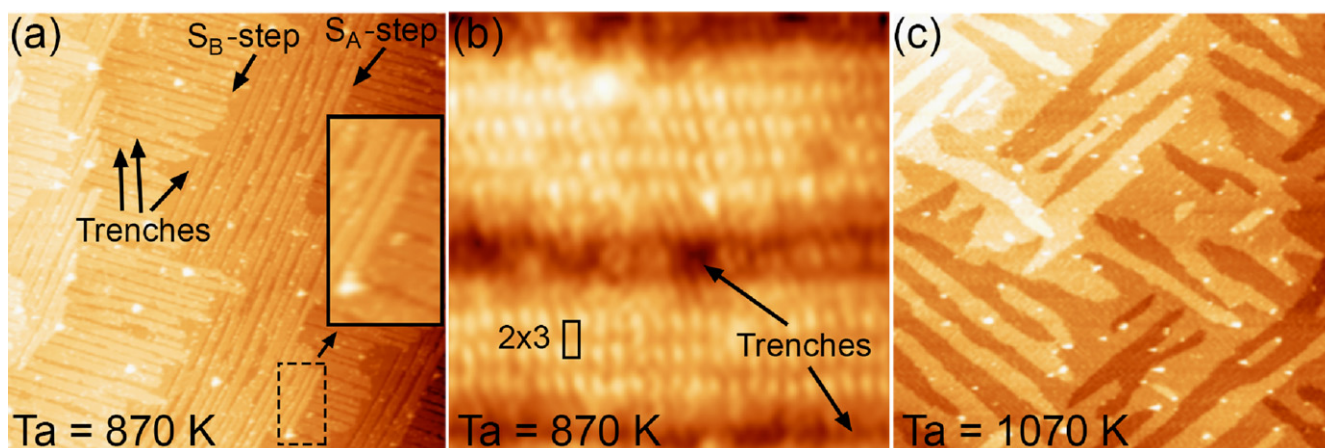


Figure 3. (a) STM image of a $400 \times 400 \text{ nm}^2$ area of the Ge(001) surface following deposition of 1 ML of Ba at RT, the subsequent annealing steps described in figure 2 and a further anneal to 870 K for 10 min. The inset (black rectangle) is a magnification of an area around an S_A -step, highlighted by the dotted rectangle, where a trench has completely separated the edge of the step from the rest of the terrace. (b) STM image of a magnified area of $20 \times 20 \text{ nm}^2$. (c) STM image of a $400 \times 400 \text{ nm}^2$ area of the surface after additional anneals to 970 and 1070 K, each for 10 min. Imaging conditions: (a) and (b) $V_s = 1 \text{ V}$, $I = 20 \text{ pA}$, (c) $V_s = -2 \text{ V}$, $I = 20 \text{ pA}$.

separations of 6–12 nm. The apparent height of individual plateaus corresponds to the height of a mono-atomic step, $0.14 \pm 0.02 \text{ nm}$, on the Ge(001) surface. The trenches themselves are 2–4 nm wide. The surface retains the initial Ge(001) terrace structure of two alternating types of terrace rotated by 90° as seen by the fact that the step edges alternate from straight (S_A -step) to ragged (S_B -step). The inset (black rectangle) in figure 3(a) is a magnification of an area around an S_A -step, highlighted by the dotted rectangle, where a trench has completely separated the edge of the step from the rest of the terrace. The measured distances between trenches correspond to 15 to 30 times the elementary Ge surface unit cell i.e. a length of up to 30 dimer rows along $[1-10]$ direction, with respect to the clean Ge(001) surface. A higher resolution image of this surface is shown in the $20 \times 20 \text{ nm}^2$ image of figure 3(b) where features with a 2×3 periodicity are observed but no evidence for the existence of pure Ge dimers. This 2×3 periodicity can be directly compared to the 2×3 units of intermixed Ba/Ge on the low coverage surface shown in figures 1(e) and (f). Moreover, the 2×3 reconstruction is strikingly similar to annealed surfaces of Sr/Si(001) [32] and Sr/Ge(001) [20].

Thus, the transformation of the surface at 870 K can be attributed to the intermixing of Ba and Ge, apparently accompanied by a volume increase which introduces compressive strain in the intermixed Ba–Ge phase layer, with the trenches providing space to relieve this strain, as has been discussed in combined STM and density functional theory studies for Sr/Ge(001) [20, 25]. Figures 3(a) and (b) demonstrate that the 770–870 K temperature range anneal step marks a crucial change in the property of the interface, where, like for the annealed Sr/Si(001) and Sr/Ge(001), the surface consists of a two-dimensional surface alloy structure, where Ba and Ge atoms co-exist in the same atomic plane.

Two further anneal steps were performed. The first, at 970 K, made little difference to the appearance of the surface

and so is not shown. The final anneal step was performed at 1070 K and an image of the surface is shown in figure 3(c). The appearance has again changed considerably although comparison with the Sr/Ge(001) [20] experiments suggests the surface retains two-dimensional alloy nature. The well defined trench structures have been replaced by non-uniform anisotropic plateaus with less well defined step edges.

4. Conclusions

In summary, through studying the adsorption of Ba on Ge(001) at low and high coverages and observing the effects of thermal annealing on these surfaces we have determined: (1) the adlayer formed by Ba deposition at RT and the subsequent surfaces formed by annealing up to temperatures of 770 K can be generically described as existing in an *on-top adsorption phase*, with no significant inter-mixing of the Ba with the underlying Ge surface; (2) the energy provided by thermal anneals up to 770 K allow the surface atoms to order into more energetically favourable structures, with some Ba desorption, which consist of nanolines rather than clusters and result in a more open surface structure with an increasing (but still small) area of the underlying Ge surface exposed; (3) annealing to 870 K and above results in the formation of a *two-dimensional alloy phase* with the Ba and Ge atoms intermixed in the surface layer; (4) at high Ba coverage, the surface strain in the alloy phase surface is relieved through the formation of large trenches which effect the step/terrace morphology which is in-turn dependent on the anneal temperature at 870 K and above. We find some similarities with comparable adsorption systems e.g. after low coverage Ba adsorption on Si(001), both Ba nanolines and local 2×3 structures of incorporated Ba were seen on the surface [26], however these were formed during Ba adsorption at 1170 K and the two phases were seen to coexist. For 0.5 monolayer

Sr layers deposited on Si(001) it was found that RT adsorption produces an on-top adsorption phase where as depositing at 920 K results in the incorporation of the Sr into the surface layer [32]. Our findings provide a recipe for the formation of Ba/Ge(001) interfaces for device applications. A separated Ba/Ge interface is likely to be desirable if the Ba–Ge interface is to promote physical or electrical isolation between the Ge surface and any subsequently deposited overlayer whereas a mixed Ba–Ge interface would promote the enhancement of electrical conductivity across the interface. Further photoemission studies, including angle-resolved ultraviolet photoelectron spectroscopy, are currently ongoing in our laboratory to corroborate the STM detected on-top adsorption phase (below 770 K) and two-dimensional alloy phase (above 870 K) by chemical state analysis as well as surface electronic band structure studies; in addition photoluminescence studies will be carried out to evaluate the influence of the two above described Ba adlayer states as potential passivation schemes to suppress surface recombination effects on *n*-doped Ge(001) surfaces.

Acknowledgments

WK and NJC acknowledge EPSRC grant EP/I02865X/1 and WK thanks IHP Frankfurt/Oder (Germany) for hospitality. WK, MWR and RC acknowledge the Polish Ministry of Science and Higher Education for support (project No. N-N202-195840).

References

- [1] Claeys C and Simoen E 2007 *Germanium-Based Technologies: From Materials to Devices* (Amsterdam: Elsevier)
- [2] Jia F, Woo R, Shulu C, Yaocheng L, Griffin P B and Plummer J D 2007 P-channel germanium FinFET based on rapid melt growth *IEEE Electron Device Lett.* **28** 637–9
- [3] Feng D et al 2009 High-speed Ge photodetector monolithically integrated with large cross-section silicon-on-insulator waveguide *Appl. Phys. Lett.* **95** 261105
- [4] Wang J and Lee S 2011 Ge-photodetectors for Si-based optoelectronic integration *Sensors* **11** 696–718
- [5] Soref R, Sun G and Cheng H H 2012 Franz–Keldysh electro-absorption modulation in germanium–tin alloys *J. Appl. Phys.* **111** 123113
- [6] Camacho-Aguilera R E, Cai Y, Patel N, Bessette J T, Romagnoli M, Kimerling L C and Michel J 2012 An electrically pumped germanium laser *Opt. Express* **20** 11316–20
- [7] Masini G, Sahni S, Capellini G, Witzens J and Gunn C 2008 High-speed near infrared optical receivers based on Ge waveguide photodetectors integrated in a CMOS process *Adv. Opt. Technol.* **2008** 196572
- [8] Na H J et al 2008 Effective surface passivation methodologies for high performance germanium metal oxide semiconductor field effect transistors *Appl. Phys. Lett.* **93** 192115
- [9] Scappucci G, Capellini G, Lee W C T and Simmons M Y 2009 Atomic-scale patterning of hydrogen terminated Ge (001) by scanning tunnelling microscopy *Nanotechnology* **20** 495302
- [10] Xie R, Phung T H, Yu M and Zhu C 2010 Effective surface passivation by novel SiH₄–NH₃ treatment and BTI characteristics on interface-engineered high-mobility HfO₂-gated Ge pMOSFETs *IEEE Trans. Electron Devices* **57** 1399–407
- [11] Reiner J W, Kolpak A M, Segal Y, Garrity K F, Ismail-Beigi S, Ahn C H and Walker F J 2010 Crystalline oxides on silicon *Adv. Mater.* **22** 2919–38
- [12] Chawanda A, Nyamhere C, Auret F D, Mtangi W, Hlatshwayo T T, Diale M and Nel J M 2009 Thermal stability study of palladium and cobalt Schottky contacts on *n*-Ge (100) and defects introduced during contacts fabrication and annealing process *Phys. B: Condens. Matter* **404** 4482–4
- [13] Chawanda A, Nyamhere C, Auret F D, Mtangi W, Diale M and Nel J M 2010 Comparison of metal schottky contacts on *n*-Ge (100) at different annealing temperatures *Phys. Status Solidi C* **7** 248–51
- [14] Grzela T, Koczorowski W, Capellini G, Czajka R, Radny M W, Curson N J, Schofield S R, Schubert M A and Schroeder T 2014 Interface and nanostructure evolution of cobalt germanides on Ge(001) *J. Appl. Phys.* **115** 074307
- [15] Lietsen R R, Afanas'ev V V, Thoan N H, Degroote S, Walukiewicz W and Borghs G 2011 Mechanisms of schottky barrier control on *n*-type germanium using Ge₃N₄ interlayers *J. Electrochem. Soc.* **158** H358–62
- [16] Abel S, Sousa M, Rossel C, Caimi D, Rossell M D, Erni R, Fompeyrine J and Marchiori C 2013 Controlling tetragonality and crystalline orientation in BaTiO₃ nanolayers grown on Si *Nanotechnology* **24** 285701
- [17] McKee R A, Walker F J and Chisholm M F 1998 Crystalline oxides on silicon: the first five monolayers *Phys. Rev. Lett.* **81** 3014–7
- [18] McKee R A, Walker F J and Chisholm M F 2001 Physical structure and inversion charge at a semiconductor interface with a crystalline oxide *Science* **293** 468–71
- [19] Niu G, Zaumseil P, Schubert M A, Zoellner M H, Dabrowski J and Schroeder T 2013 Lattice-matched epitaxial ternary Pr_xY_{2-x}O₃ films on SrO-passivated Si (001): interface engineering and crystallography tailoring *Appl. Phys. Lett.* **102** 011906
- [20] Lukanov B R, Reiner J W, Walker F J, Ahn C H and Altman E I 2011 Formation of alkaline-earth template layers on Ge(100) for oxide heteroepitaxy: self-organization of ordered islands and trenches *Phys. Rev. B* **84** 075330
- [21] Merckling C, Saint-Girons G, Botella C, Hollinger G, Heyns M, Dekoster J and Caymax M 2011 Molecular beam epitaxial growth of BaTiO₃ single crystal on Ge-on-Si(001) substrates *Appl. Phys. Lett.* **98** 092901
- [22] Radny M W, Shah G A, Schofield S R, Smith P V and Curson N J 2008 Valence surface electronic states on Ge (001) *Phys. Rev. Lett.* **100** 246807
- [23] Cattoni A, Bertacco R, Riva M, Cantoni M, Ciccacci F, Von Känel H and Norga G J 2006 Effect of Ba termination layer on chemical and electrical passivation of Ge(100) surfaces *Mater. Sci. Semicond. Process.* **9** 701–5
- [24] Lukanov B R, Garrity K F, Ismail-Beigi S and Altman E I 2012 Deciphering the atomic structure of a complex Sr/Ge (100) phase via scanning tunneling microscopy and first-principles calculations *Phys. Rev. B* **85** 195316
- [25] Lukanov B R, Garrity K F, Ismail-Beigi S and Altman E I 2014 Formation and atomic structure of ordered Sr-induced nanostrips on Ge(100) *Phys. Rev. B* **89** 155319
- [26] Hu X et al 2000 The (3 × 2) phase of Ba adsorption on Si(001)-2 × 1 *Surf. Sci.* **445** 256–66
- [27] Zandvliet H J W 2003 The Ge(001) surface *Phys. Rep.* **388** 1–40
- [28] Horcas I, Fernández R, Gómez-Rodríguez J M, Colchero J, Gómez-Herrero J and Baro A M 2007 WSXM: a software

- for scanning probe microscopy and a tool for nanotechnology *Rev. Sci. Instrum.* **78** 013705
- [29] Hu X *et al* 2000 Barium adsorption on Si(100)-(2 × 1) at room temperature: a bi-polar scanning tunneling microscopy study *Surf. Sci.* **457** L391–6
- [30] Hasegawa Y, Kamiya I, Hashizume T, Sakurai T, Tochihara M, Kubota M and Murata Y 1990 Adsorption of Li (K) on the Si(001)-(2 × 1) surface: scanning-tunneling-microscopy study *Phys. Rev. B.* **41** 9688
- [31] Pyykko P and Atsumi M 2009 Molecular double-bond covalent radii for elements Li–E112 *Chem. Eur. J.* **15** 12770–9
- [32] Reiner J, Garrity K, Walker F, Ismail-Beigi S and Ahn C 2008 Role of strontium in oxide epitaxy on silicon (001) *Phys. Rev. Lett.* **101** 105503